PHYSICAL REVIEW D **75,** 111103(R) (2007)

Measurement of the top-quark mass using missing E_T + jets events with secondary vertex *b*-tagging at CDF II

T. Aaltonen,[23] A. Abulencia,[24] J. Adelman,[13] T. Affolder,[10] T. Akimoto,[55] M. G. Albrow,[17] S. Amerio,[43] D. Amidei,[35] A. Anastassov,[52] K. Anikeev,[17] A. Annovi,[19] J. Antos,[14] M. Aoki,[55] G. Apollinari,[17] T. Arisawa,[57] A. Artikov,[15] W. Ashmanskas,[17] A. Attal,[3] A. Aurisano,[42] F. Azfar,[42] P. Azzi-Bacchetta,[43] P. Azzurri,[46] N. Bacchetta,[43] W. Badgett,[17] A. Barbaro-Galtieri,[29] V. E. Barnes,[48] B. A. Barnett,[25] S. Baroiant,[7] V. Bartsch,[31] G. Bauer,[33] P.-H. Beauchemin,[34] F. Bedeschi,[46] S. Behari,[25] G. Bellettini,[46] J. Bellinger,[59] A. Belloni,[33] D. Benjamin,[16] A. Beretvas,[17] J. Beringer,[29] T. Berry,[30] A. Bhatti,[50] M. Binkley,[17] D. Bisello,[43] I. Bizjak,[31] R. E. Blair,[2] C. Blocker,[6] B. Blumenfeld,[25] A. Bocci,[16] A. Bodek,[49] V. Boisvert,[49] G. Bolla,[48] A. Bolshov,[33] D. Bortoletto,[48] J. Boudreau,[47] A. Boveia,[10] B. Brau,[10] L. Brigliadori,[5] C. Bromberg,[36] E. Brubaker,[13] J. Budagov,[15] H. S. Budd,[49] S. Budd,[24] K. Burkett,[17] G. Busetto,[43] P. Bussey,[21] A. Buzatu,[34] K. L. Byrum,[2] S. Cabrera,[16,r] M. Campanelli,[20] M. Campbell,[35] F. Canelli,[17] A. Canepa,[45] S. Carillo,[18,j] D. Carlsmith,[59] R. Carosi,[46] S. Carron,[34] B. Casal,[11] M. Casarsa,[54] A. Castro,[5] P. Catastini,[46] D. Cauz,[54] M. Cavalli-Sforza,[3] A. Cerri,[29] L. Cerrito,[31,n] S. H. Chang,[28] Y. C. Chen,[1] M. Chertok,[7] G. Chiarelli,[46] G. Chlachidze,[17] F. Chlebana,[17] I. Cho,[28] K. Cho,[28] D. Chokheli,[15] J. P. Chou,[22] G. Choudalakis,[33] S. H. Chuang,[52] K. Chung,[12] W. H. Chung,[59] Y. S. Chung,[49] M. Cilijak,[46] C. I. Ciobanu,[24] M. A. Ciocci,[46] A. Clark,[20] D. Clark,[6] M. Coca,[16] G. Compostella,[43] M. E. Convery,[50] J. Conway,[7] B. Cooper,[31] K. Copic,[35] M. Cordelli,[19] G. Cortiana,[43] F. Crescioli,[46] C. Cuenca Almenar,[7,r] J. Cuevas,[11,m] R. Culbertson,[17] J. C. Cully,[35] S. DaRonco,[43] M. Datta,[17] S. D'Auria,[21] T. Davies,[21] D. Dagenhart,[17] P. de Barbaro,[49] S. De Cecco,[51] A. Deisher,[29] G. De Lentdecker,[49,d] G. De Lorenzo,[3] M. Dell'Orso,[46] F. Delli Paoli,[43] L. Demortier,[50] J. Deng,[16] M. Deninno,[5] D. De Pedis,[51] P. F. Derwent,[17] G. P. Di Giovanni,[44] C. Dionisi,[51] B. Di Ruzza,[54] J. R. Dittmann,[4] M. D'Onofrio,[3] C. Dörr,[26] S. Donati,[46] P. Dong,[8] J. Donini,[43] T. Dorigo,[43] S. Dube,[52] J. Efron,[39] R. Erbacher,[7] D. Errede,[24] S. Errede,[24] R. Eusebi,[17] H. C. Fang,[29] S. Farrington,[30] I. Fedorko,[46] W. T. Fedorko,[13] R. G. Feild,[60] M. Feindt,[26] J. P. Fernandez,[32] R. Field,[18] G. Flanagan,[48] R. Forrest,[7] S. Forrester,[7] M. Franklin,[22] J. C. Freeman,[29] I. Furic,[13] M. Gallinaro,[50] J. Galyardt,[12] J. E. Garcia,[46] F. Garberson,[10] A. F. Garfinkel,[48] C. Gay,[60] H. Gerberich,[24] D. Gerdes,[35] S. Giagu,[51] P. Giannetti,[46] K. Gibson,[47] J. L. Gimmell,[49] C. Ginsburg,[17] N. Giokaris,[15,b] M. Giordani,[54] P. Giromini,[19] M. Giunta,[46] G. Giurgiu,[25] V. Glagolev,[15] D. Glenzinski,[17] M. Gold,[37] N. Goldschmidt,[18] J. Goldstein,[42,c] A. Golossanov,[17] G. Gomez,[11] G. Gomez-Ceballos,[33] M. Goncharov,[53] O. González,[32] I. Gorelov,[37] A. T. Goshaw,[16] K. Goulianos,[50] A. Gresele,[43] S. Grinstein,[22] C. Grosso-Pilcher,[13] R. C. Group,[17] U. Grundler,[24] J. Guimaraes da Costa,[22] Z. Gunay-Unalan,[36] C. Haber,[29] K. Hahn,[33] S. R. Hahn,[17] E. Halkiadakis,[52] A. Hamilton,[20] B.-Y. Han,[49] J. Y. Han,[49] R. Handler,[59] F. Happacher,[19] K. Hara,[55] D. Hare,[52] M. Hare,[56] S. Harper,[42] R. F. Harr,[58] R. M. Harris,[17] M. Hartz,[47] K. Hatakeyama,[50] J. Hauser,[8] C. Hays,[42] M. Heck,[26] A. Heijboer,[45] B. Heinemann,[29] J. Heinrich,[45] C. Henderson,[33] M. Herndon,[59] J. Heuser,[26] D. Hidas,[16] C. S. Hill,[10,c] D. Hirschbuehl,[26] A. Hocker,[17] A. Holloway,[22] S. Hou,[1] M. Houlden,[30] S.-C. Hsu,[9] B. T. Huffman,[42] R. E. Hughes,[39] U. Husemann,[60] J. Huston,[36] J. Incandela,[10] G. Introzzi,[46] M. Iori,[51] A. Ivanov,[7] B. Iyutin,[33] E. James,[17] D. Jang,[52] B. Jayatilaka,[16] D. Jeans,[51] E. J. Jeon,[28] S. Jindariani,[18] W. Johnson,[7] M. Jones,[48] K. K. Joo,[28] S. Y. Jun,[12] J. E. Jung,[28] T. R. Junk,[24] T. Kamon,[53] P. E. Karchin,[58] Y. Kato,[41] Y. Kemp,[26] R. Kephart,[17] U. Kerzel,[26] V. Khotilovich,[53] B. Kilminster,[39] D. H. Kim,[28] H. S. Kim,[28] J. E. Kim,[28] M. J. Kim,[17] S. B. Kim,[28] S. H. Kim,[55] Y. K. Kim,[13] N. Kimura,[55] L. Kirsch,[6] S. Klimenko,[18] M. Klute,[33] B. Knuteson,[33] B. R. Ko,[16] K. Kondo,[57] D. J. Kong,[28] J. Konigsberg,[18] A. Korytov,[18] A. V. Kotwal,[16] A. C. Kraan,[45] J. Kraus,[24] M. Kreps,[26] J. Kroll,[45] N. Krumnack,[4] M. Kruse,[16] V. Krutelyov,[10] T. Kubo,[55] S. E. Kuhlmann,[2] T. Kuhr,[26] N. P. Kulkarni,[58] Y. Kusakabe,[57] S. Kwang,[13] A. T. Laasanen,[48] S. Lai,[34] S. Lami,[46] S. Lammel,[17] M. Lancaster,[31] R. L. Lander,[7] K. Lannon,[39] A. Lath,[52] G. Latino,[46] I. Lazzizzera,[43] T. LeCompte,[2] J. Lee,[49] J. Lee,[28] Y. J. Lee,[28] S. W. Lee,[53,p] R. Lefèvre,[20] N. Leonardo,[33] S. Leone,[46] S. Levy,[13] J. D. Lewis,[17] C. Lin,[60] C. S. Lin,[17] M. Lindgren,[17] E. Lipeles,[9] A. Lister,[7] D. O. Litvintsev,[17] T. Liu,[17] N. S. Lockyer,[45] A. Loginov,[60] M. Loreti,[43] R.-S. Lu,[1] D. Lucchesi,[43] P. Lujan,[29] P. Lukens,[17] G. Lungu,[18] L. Lyons,[42] J. Lys,[29] R. Lysak,[14] E. Lytken,[48] P. Mack,[26] D. MacQueen,[34] R. Madrak,[17] K. Maeshima,[17] K. Makhoul,[33] T. Maki,[23] P. Maksimovic,[25] S. Malde,[42] S. Malik,[31] G. Manca,[30] A. Manousakis,[15,b] F. Margaroli,[5] R. Marginean,[17] C. Marino,[26] C. P. Marino,[24] A. Martin,[60] M. Martin,[25] V. Martin,[21,h] M. Martínez,[3] R. Martínez-Ballarín,[32] T. Maruyama,[55] P. Mastrandrea,[51] T. Masubuchi,[55] H. Matsunaga,[55] M. E. Mattson,[58] R. Mazini,[34] P. Mazzanti,[5] K. S. McFarland,[49] P. McIntyre,[53] R. McNulty,[30,g] A. Mehta,[30] P. Mehtala,[23] S. Menzemer,[11,i] A. Menzione,[46] P. Merkel,[48] C. Mesropian,[50] A. Messina,[36] T. Miao,[17] N. Miladinovic,[6] J. Miles,[33] R. Miller,[36] C. Mills,[10] M. Milnik,[26] A. Mitra,[1] G. Mitselmakher,[18] A. Miyamoto,[27] S. Moed,[20] N. Moggi,[5] B. Mohr,[8] C. S. Moon,[28] R. Moore,[17] M. Morello,[46] P. Movilla Fernandez,[29] J. Mülmenstädt,[29] A. Mukherjee,[17] Th. Muller,[26]

R. Mumford,[25] P. Murat,[17] M. Mussini,[5] J. Nachtman,[17] A. Nagano,[55] J. Naganoma,[57] K. Nakamura,[55] I. Nakano,[40] A. Napier,[56] V. Necula,[16] C. Neu,[45] M. S. Neubauer,[9] J. Nielsen,[29,o] L. Nodulman,[2] O. Norniella,[3] E. Nurse,[31] S. H. Oh,[16] Y. D. Oh,[28] I. Oksuzian,[18] T. Okusawa,[41] R. Oldeman,[30] R. Orava,[23] K. Osterberg,[23] C. Pagliarone,[46] E. Palencia,[11] V. Papadimitriou,[17] A. Papaikonomou,[26] A. A. Paramonov,[13] B. Parks,[39] S. Pashapour,[34] J. Patrick,[17] G. Pauletta,[54] M. Paulini,[12] C. Paus,[33] D. E. Pellett,[7] A. Penzo,[54] T. J. Phillips,[16] G. Piacentino,[46] J. Piedra,[44] L. Pinera,[18] K. Pitts,[24] C. Plager,[8] L. Pondrom,[59] X. Portell,[3] O. Poukhov,[15] N. Pounder,[42] F. Prakoshyn,[15] A. Pronko,[17] J. Proudfoot,[2] F. Ptohos,[19,f] G. Punzi,[46] J. Pursley,[25] J. Rademacker,[42,c] A. Rahaman,[47] V. Ramakrishnan,[59] N. Ranjan,[48] I. Redondo,[32] B. Reisert,[17] V. Rekovic,[37] P. Renton,[42] M. Rescigno,[51] S. Richter,[26] F. Rimondi,[5] L. Ristori,[46] A. Robson,[21] T. Rodrigo,[11] E. Rogers,[24] S. Rolli,[56] R. Roser,[17] M. Rossi,[54] R. Rossin,[10] P. Roy,[34] A. Ruiz,[11] J. Russ,[12] V. Rusu,[13] H. Saarikko,[23] A. Safonov,[53] W. K. Sakumoto,[49] G. Salamanna,[51] O. Saltó,[3] L. Santi,[54] S. Sarkar,[51] L. Sartori,[46] K. Sato,[17] P. Savard,[34] A. Savoy-Navarro,[44] T. Scheidle,[26] P. Schlabach,[17] E. E. Schmidt,[17] M. P. Schmidt,[60] M. Schmitt,[38] T. Schwarz,[7] L. Scodellaro,[11] A. L. Scott,[10] A. Scribano,[46] F. Scuri,[46] A. Sedov,[48] S. Seidel,[37] Y. Seiya,[41] A. Semenov,[15] L. Sexton-Kennedy,[17] A. Sfyrla,[20] S. Z. Shalhout,[58] M. D. Shapiro,[29] T. Shears,[30] P. F. Shepard,[47] D. Sherman,[22] M. Shimojima,[55,l] M. Shochet,[13] Y. Shon,[59] I. Shreyber,[20] A. Sidoti,[46] P. Sinervo,[34] A. Sisakyan,[15] A. J. Slaughter,[17] J. Slaunwhite,[39] K. Sliwa,[56] J. R. Smith,[7] F. D. Snider,[17] R. Snihur,[34] M. Soderberg,[35] A. Soha,[7] S. Somalwar,[52] V. Sorin,[36] J. Spalding,[17] F. Spinella,[46] T. Spreitzer,[34] P. Squillacioti,[46] M. Stanitzki,[60] A. Staveris-Polykalas,[46] R. St. Denis,[21] B. Stelzer,[8] O. Stelzer-Chilton,[42] D. Stentz,[38] J. Strologas,[37] D. Stuart,[10] J. S. Suh,[28] A. Sukhanov,[18] H. Sun,[56] I. Suslov,[15] T. Suzuki,[55] A. Taffard,[24,q] R. Takashima,[40] Y. Takeuchi,[55] R. Tanaka,[40] M. Tecchio,[35] P. K. Teng,[1] K. Terashi,[50] J. Thom,[17,e] A. S. Thompson,[21] E. Thomson,[45] P. Tipton,[60] V. Tiwari,[12] S. Tkaczyk,[17] D. Toback,[53] S. Tokar,[14] K. Tollefson,[36] T. Tomura,[55] D. Tonelli,[46] S. Torre,[19] D. Torretta,[17] S. Tourneur,[44] W. Trischuk,[34] S. Tsuno,[40] Y. Tu,[45] N. Turini,[46] F. Ukegawa,[55] S. Uozumi,[55] S. Vallecorsa,[20] N. van Remortel,[23] A. Varganov,[35] E. Vataga,[37] F. Vazquez,[18,j] G. Velev,[17] C. Vellidis,[46,b] G. Veramendi,[24] V. Veszpremi,[48] M. Vidal,[32] R. Vidal,[17] I. Vila,[11] R. Vilar,[11] T. Vine,[31] M. Vogel,[37] I. Vollrath,[34] I. Volobouev,[29,p] G. Volpi,[46] F. Würthwein,[9] P. Wagner,[53] R. G. Wagner,[2] R. L. Wagner,[17] J. Wagner,[26] W. Wagner,[26] R. Wallny,[8] S. M. Wang,[1] A. Warburton,[34] D. Waters,[31] M. Weinberger,[53] W. C. Wester III,[17] B. Whitehouse,[56] D. Whiteson,[45] A. B. Wicklund,[2] E. Wicklund,[17] G. Williams,[34] H. H. Williams,[45] P. Wilson,[17] B. L. Winer,[39] P. Wittich,[17,e] S. Wolbers,[17] C. Wolfe,[13] T. Wright,[35] X. Wu,[20] S. M. Wynne,[30] A. Yagil,[9] K. Yamamoto,[41] J. Yamaoka,[52] T. Yamashita,[40] C. Yang,[60] U. K. Yang,[13,k] Y. C. Yang,[28] W. M. Yao,[29] G. P. Yeh,[17] J. Yoh,[17] K. Yorita,[13] T. Yoshida,[41] G. B. Yu,[49] I. Yu,[28] S. S. Yu,[17] J. C. Yun,[17] L. Zanello,[51] A. Zanetti,[54] I. Zaw,[22] X. Zhang,[24] J. Zhou,[52] and S. Zucchelli[5]

(CDF Collaboration)[a]

[1]*Institute of Physics, Academia Sinica, Taipei, Taiwan 11529, Republic of China*
[2]*Argonne National Laboratory, Argonne, Illinois 60439, USA*
[3]*Institut de Fisica d'Altes Energies, Universitat Autonoma de Barcelona, E-08193, Bellaterra (Barcelona), Spain*
[4]*Baylor University, Waco, Texas 76798, USA*
[5]*Istituto Nazionale di Fisica Nucleare, University of Bologna, I-40127 Bologna, Italy*
[6]*Brandeis University, Waltham, Massachusetts 02254, USA*
[7]*University of California, Davis, Davis, California 95616, USA*
[8]*University of California, Los Angeles, Los Angeles, California 90024, USA*
[9]*University of California, San Diego, La Jolla, California 92093, USA*
[10]*University of California, Santa Barbara, Santa Barbara, California 93106, USA*
[11]*Instituto de Fisica de Cantabria, CSIC-University of Cantabria, 39005 Santander, Spain*
[12]*Carnegie Mellon University, Pittsburgh, Pennsylvania 15213, USA*
[13]*Enrico Fermi Institute, University of Chicago, Chicago, Illinois 60637, USA*
[14]*Comenius University, 842 48 Bratislava, Slovakia and Institute of Experimental Physics, 040 01 Kosice, Slovakia*
[15]*Joint Institute for Nuclear Research, RU-141980 Dubna, Russia*
[16]*Duke University, Durham, North Carolina 27708, USA*
[17]*Fermi National Accelerator Laboratory, Batavia, Illinois 60510, USA*
[18]*University of Florida, Gainesville, Florida 32611, USA*
[19]*Laboratori Nazionali di Frascati, Istituto Nazionale di Fisica Nucleare, I-00044 Frascati, Italy*
[20]*University of Geneva, CH-1211 Geneva 4, Switzerland*
[21]*Glasgow University, Glasgow G12 8QQ, United Kingdom*
[22]*Harvard University, Cambridge, Massachusetts 02138, USA*
[23]*Division of High Energy Physics, Department of Physics, University of Helsinki, FIN-00014, Helsinki, Finland and Helsinki Institute of Physics, FIN-00014, Helsinki, Finland*

[24]University of Illinois, Urbana, Illinois 61801, USA
[25]The Johns Hopkins University, Baltimore, Maryland 21218, USA
[26]Institut für Experimentelle Kernphysik, Universität Karlsruhe, 76128 Karlsruhe, Germany
[27]High Energy Accelerator Research Organization (KEK), Tsukuba, Ibaraki 305, Japan
[28]Center for High Energy Physics, Kyungpook National University, Taegu 702-701, Korea;
Seoul National University, Seoul 151-742, Korea; and SungKyunKwan University, Suwon 440-746, Korea
[29]Ernest Orlando Lawrence Berkeley National Laboratory, Berkeley, California 94720, USA
[30]University of Liverpool, Liverpool L69 7ZE, United Kingdom
[31]University College London, London WC1E 6BT, United Kingdom
[32]Centro de Investigaciones Energeticas Medioambientales y Tecnologicas, E-28040 Madrid, Spain
[33]Massachusetts Institute of Technology, Cambridge, Massachusetts 02139, USA
[34]Institute of Particle Physics, McGill University, Montréal, Canada H3A 2T8 and University of Toronto, Toronto, Canada M5S 1A7
[35]University of Michigan, Ann Arbor, Michigan 48109, USA
[36]Michigan State University, East Lansing, Michigan 48824, USA
[37]University of New Mexico, Albuquerque, New Mexico 87131, USA
[38]Northwestern University, Evanston, Illinois 60208, USA
[39]The Ohio State University, Columbus, Ohio 43210, USA
[40]Okayama University, Okayama 700-8530, Japan
[41]Osaka City University, Osaka 588, Japan
[42]University of Oxford, Oxford OX1 3RH, United Kingdom
[43]University of Padova, Istituto Nazionale di Fisica Nucleare, Sezione di Padova-Trento, I-35131 Padova, Italy
[44]LPNHE, Universite Pierre et Marie Curie/IN2P3-CNRS, UMR7585, Paris, F-75252 France
[45]University of Pennsylvania, Philadelphia, Pennsylvania 19104, USA
[46]Istituto Nazionale di Fisica Nucleare Pisa, Universities of Pisa, Siena and Scuola Normale Superiore, I-56127 Pisa, Italy
[47]University of Pittsburgh, Pittsburgh, Pennsylvania 15260, USA
[48]Purdue University, West Lafayette, Indiana 47907, USA
[49]University of Rochester, Rochester, New York 14627, USA
[50]The Rockefeller University, New York, New York 10021, USA
[51]Istituto Nazionale di Fisica Nucleare, Sezione di Roma 1, University of Rome "La Sapienza," I-00185 Roma, Italy
[52]Rutgers University, Piscataway, New Jersey 08855, USA
[53]Texas A&M University, College Station, Texas 77843, USA
[54]Istituto Nazionale di Fisica Nucleare, University of Trieste/Udine, Italy
[55]University of Tsukuba, Tsukuba, Ibaraki 305, Japan
[56]Tufts University, Medford, Massachusetts 02155, USA
[57]Waseda University, Tokyo 169, Japan
[58]Wayne State University, Detroit, Michigan 48201, USA
[59]University of Wisconsin, Madison, Wisconsin 53706, USA
[60]Yale University, New Haven, Connecticut 06520, USA
(Received 11 May 2007; published 29 June 2007)

We present a measurement of the top-quark mass in $p\bar{p}$ collisions at $\sqrt{s} = 1.96$ TeV which uses events with an inclusive signature of missing transverse energy and jets. The event selection is sensitive to $t\bar{t} \rightarrow W^+bW^-\bar{b} \rightarrow l\nu bqq'\bar{b}$ independent of the lepton flavor and results in a large acceptance for $W \rightarrow \tau\nu$ decays. All-hadronic $t\bar{t}$ decays and events with identified electrons or muons are vetoed to provide a statistically independent sample with respect to all previous measurements. The top-quark mass is inferred from the distribution of the scalar sum of all jet transverse energies and the missing transverse energy. Using 311 pb^{-1} of integrated luminosity recorded by the Collider Detector at Fermilab, we measure a top-quark mass $m_t = 172.3^{+10.8}_{-9.6}(\text{stat}) \pm 10.8(\text{syst})$ GeV$/c^2$. While the uncertainty on m_t is larger than that of other measurements, the result is statistically uncorrelated with those of other methods and thus can help to reduce the overall m_t uncertainty when combined with other existing measurements.

DOI: 10.1103/PhysRevD.75.111103 PACS numbers: 12.15.Ff, 13.85.Ni, 14.65.Ha

[a]With visitors from
[b]University of Athens,
[c]University of Bristol,
[d]University Libre de Bruxelles,
[e]Cornell University,
[f]University of Cyprus,
[g]University of Dublin,
[h]University of Edinburgh,
[i]University of Heidelberg,
[j]Universidad Iberoamericana,
[k]University of Manchester,
[l]Nagasaki Institute of Applied Science,
[m]University de Oviedo,
[n]University of London, Queen Mary College,
[o]University of California Santa Cruz,
[p]Texas Tech University,
[q]University of California Irvine,
[r]IFIC(CSIC-Universitat de Valencia).

The top-quark mass, m_t, is an important free parameter in the standard model (SM) of particle physics. Being roughly 40 times larger than the mass of its weak isospin partner, the b quark, m_t gives large contributions to electroweak radiative corrections which, when connected to precision electroweak measurements, can be used to derive constraints on the masses of the yet-unobserved Higgs boson [1], and of particles belonging to some SM extensions [2]. At the Tevatron $p\bar{p}$ collider top quarks are produced mainly in pairs through quark-antiquark annihilation and gluon-gluon fusion processes. Because the Cabibbo-Kobayashi-Maskawa matrix element V_{tb} [3] is close to unity, the SM top-quark decays to a W boson and a b quark almost 100% of the time. The final state of a top-quark pair thus includes two W bosons and two b-quark jets. When only one W decays leptonically, the $t\bar{t}$ event typically contains a charged lepton, missing transverse energy ($\not\!\!E_T$) from the undetected neutrino [4], and four high-transverse-energy jets, two of which originate from b quarks.

Recently the CDF Collaboration has reported precision m_t measurements using $t\bar{t}$ events containing identified high-p_T leptons (e, μ) [5] and all-hadronic decays [6]. In this paper we describe a top-quark mass measurement which uses events collected by a multijet trigger and selected by requiring an inclusive high-p_T neutrino signature, consisting of large $\not\!\!E_T$. Events containing identified high-p_T electrons or muons ($E_T^e \geq 20$ GeV, $P_T^\mu \geq 20$ GeV$/c$), as defined in [7], are removed in order to increase the relative contribution of $W \rightarrow \tau\nu$ decays and provide a statistically independent sample with respect to other lepton-based measurements [5]. All-hadronic $t\bar{t}$ decays are discarded by the $\not\!\!E_T$ requirement so that orthogonality with respect to the all-hadronic mass sample is ensured [6,8]. Unlike previous analyses based on the identification of $W \rightarrow e\nu(\mu\nu)$ and $W \rightarrow qq'$ decays, our event selection does not permit a full kinematical reconstruction of the $t\bar{t}$ final state. For this reason, the top-quark mass is derived from the H_T distribution, where H_T is defined as the scalar sum of all jet transverse energies and the $\not\!\!E_T$.

Results reported in this paper are obtained using 311 pb^{-1} of integrated luminosity from $p\bar{p}$ collisions at $\sqrt{s} = 1.96$ TeV, recorded by the Collider Detector at Fermilab (CDF II). The CDF II detector is described in detail elsewhere [9]. It consists of a magnetic spectrometer surrounded by a calorimeter and muon system. The momenta of charged particles are measured up to a pseudorapidity of $|\eta| = 1.0$ in a cylindrical drift chamber, which is inside a 1.4 T superconducting solenoidal magnet. Silicon microstrip vertex detectors, located immediately outside the beampipe, provide precise track reconstruction useful for vertexing and extend the coverage of the tracking system up to $|\eta| = 2.0$. Electromagnetic and hadronic sampling calorimeters, arranged in a projective-tower geometry, surround the tracking systems and measure the energy and direction of electrons, photons, and jets in the range $|\eta| < 3.6$. In addition, the good Hermiticity provided by the calorimeter allows the detection of high-p_T neutrinos by the measurement of the $\not\!\!E_T$. Muon systems outside the calorimeters allow the reconstruction of track segments for penetrating particles. The beam luminosity is determined using gas Cherenkov counters surrounding the beam pipe, which measure the average number of inelastic $p\bar{p}$ collisions per bunch crossing.

The data sample used in this analysis is collected by a multijet trigger which requires four or more $E_T \geq 15$ GeV clusters of contiguous calorimeter towers, and a scalar sum of transverse energy clustered in the calorimeter of $\sum E_T \geq 125$ GeV. The initial data sample consists of 4.2×10^6 events and is further reduced offline by the application of kinematical and topological requirements aimed at optimizing the $t\bar{t}$ signal significance [10]. Briefly, we require at least four jets having $E_T \geq 15$ GeV and $|\eta| \leq 2.0$; $\not\!\!E_T$ significance, $\not\!\!E_T^{\rm sig}$, greater than 4.0 GeV$^{1/2}$, where $\not\!\!E_T^{\rm sig}$ is defined as $\not\!\!E_T/\sqrt{\sum E_T}$; and a minimum separation in azimuthal angle between the $\not\!\!E_T$ and the closest jet, $\min\Delta\phi \geq 0.4$ rad. In our selection, jets are identified as groups of calorimeter tower energy deposits within a cone of radius $\Delta R = \sqrt{\Delta\phi^2 + \Delta\eta^2} \leq 0.4$, and their energies are corrected for calorimeter nonlinearity, losses in the gaps between towers, multiple interactions, and particle response calibrations [11]. This selection reduces the data sample to 597 events, with a signal to background ratio $S/B \sim 1/5$. In order to further increase the expected S/B ratio and reject background events with only light quark or gluon jets, b-quark jets (''b tags'') are identified by the reconstruction of secondary decay vertices using the SECVTX algorithm, as in [7]. After these selections and the requirement of at least one b-tagged jet, we observe 106 events with $S/B \sim 1$; about 44% of the signal acceptance is accounted for by $t\bar{t} \rightarrow W^+bW^-\bar{b} \rightarrow \tau\nu bqq'\bar{b}$ decays, while the remaining $t\bar{t}$ content is dominated by $e(\mu)$ + jets events, in which the lepton fails the standard high-p_T identification cuts.

Background events with b tags arise from QCD heavy flavor production, electroweak production of W bosons associated with heavy flavor jets, and from false identification by the SECVTX algorithm. The overall number of background b tags in the final data sample, and their corresponding kinematical distributions, are estimated using a per jet parameterization of the b-tagging probability derived from the multijet sample. For the parameterization, we use events with exactly three jets, having $E_T \geq 15$ GeV and $|\eta| \leq 1.0$, where the $t\bar{t}$ content is negligible. The parameterization exploits the b-tag rate dependencies on the jet E_T, the charged track multiplicity inside the jet cone, and the projection of the $\not\!\!E_T$ along the jet direction in the transverse plane, which is defined by $\not\!\!E_T^{\rm prj} = \not\!\!E_T \cos\Delta\phi(\not\!\!E_T, \text{jet})$. The extrapolation of the 3-jet b-tagging probability to higher jet multiplicity events,

and the capability of the parameterization to track sample composition changes introduced by the kinematical selection, are checked using ≥ 4-jet data samples depleted of signal content, as described elsewhere [10]: (a) data before the optimized kinematical selection on $\not\!\!E_T^{\rm sig}$ and $\min\Delta\phi(\not\!\!E_T, \text{jets})$; (b) $\not\!\!E_T^{\rm sig} \leq 3.0\ \text{GeV}^{1/2}$, $\min\Delta\phi(\not\!\!E_T, \text{jets}) \geq 0.3$ rad; and (c) $\not\!\!E_T^{\rm sig} \geq 3.0\ \text{GeV}^{1/2}$, $\min\Delta\phi(\not\!\!E_T, \text{jets}) \leq 0.3$ rad. As a result, the b-tag rate parameterization is found to predict the number of background b tags, and the shape of their corresponding kinematical distributions, to within 10% in the $4 \leq N_{\rm jet} \leq 6$ region, where 96.4% of the $t\bar{t}$ signal is expected after the optimized kinematical selection. Figure 1 shows the comparison between expected and observed background H_T distributions in the data control samples (a), (b), and (c). The expected H_T distributions are derived from the b-tag rate parameterization applied to each jet belonging to a given data sample, before b-jet identification requirements. The observed H_T distributions receive one entry per b-tagged jet for a proper normalization with the expectation. The normalization and shape of the observed and expected distributions are in good agreement for all control samples.

The final data sample, after the optimized kinematical selection and the additional requirement of at least one b-tagged jet, contains a total of 127 b-tagged jets. The number of b-tagged jets yielded by background processes in that sample is expected to be $n_b^{\rm exp} = 57.4 \pm 8.1$. The excess in the number of b tags is ascribed to top-quark pair production. We derive a measurement of the top-quark mass from the observed H_T distribution. The H_T distribution from the selected data is fit to the sum of signal and background H_T contribution parameterizations using an unbinned likelihood technique. Probability density functions are determined for signal, as a function of m_t, and for background events by fitting a functional form from the corresponding H_T distributions (templates). For consistency with our per jet background prediction method, the H_T distributions from data and simulated signal events receive one entry per b-tagged jet.

We calibrate our method using events with inclusive $t\bar{t}$ decays generated with different input values of m_t ranging from 150 to 200 GeV/c^2, in steps of 2.5 GeV/c^2. These events are simulated using the HERWIG [12] generator in conjunction with the CTEQ5L [13] parton distribution functions (PDFs), QQ [14] for the modeling of b and c hadron decays, and a full simulation of the CDF II detector [15,16]. They are then subjected to the same selection as the recorded events. The H_T distributions, derived at discrete values of the top-quark mass, are parameterized by a continuous functional form as a function of m_t in order to smooth the distributions and interpolate between the templates. For any given m_t the probability to observe a particular H_T value is specified by a normalized Pearson type IV function [17], in which the parameters are assumed to be linearly dependent on m_t. The best parameterization is determined by a simultaneous binned likelihood fit to all signal templates. In Fig. 2, four signal templates are shown overlaid with their corresponding parameterization.

For background, the H_T distribution is derived from the b-tag rate parameterization applied to jets belonging to the kinematically selected data sample, before b-jet identification requirements. It has no dependence on the top-quark mass, except from a procedure adopted to subtract the expected signal content ($\sim 15\%$ for $m_t = 172.5\ \text{GeV}/c^2$). The arbitrary m_t choice in the subtraction procedure is accounted for in the background shape systematic uncertainty. A single probability density function, defined as the sum of a gamma function and two Gaussians, is used to fit the background H_T template, as shown in Fig. 3.

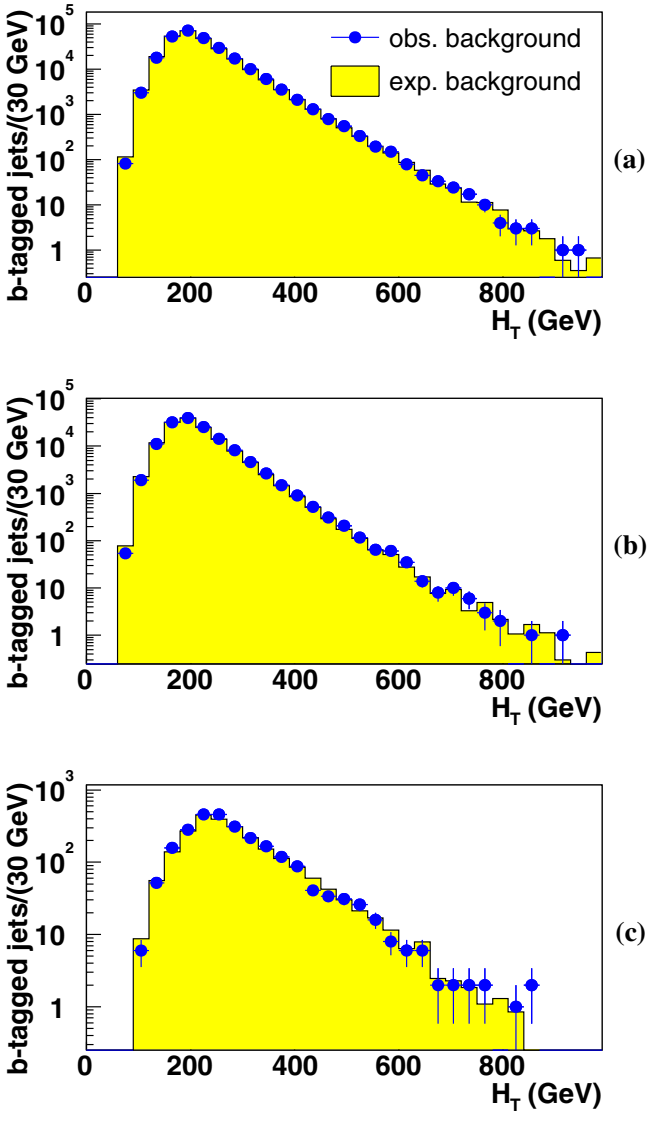

FIG. 1 (color online). Observed and expected H_T background distributions in data control samples depleted of signal contamination; see text for details.

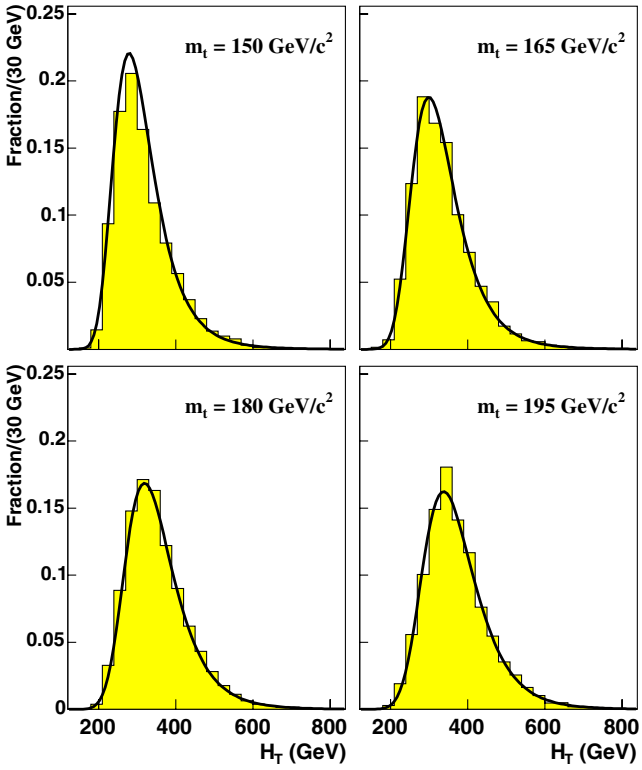

FIG. 2 (color online). Four H_T signal templates with m_t ranging from 150 to 195 GeV/c^2. Overlaid are the fitted parameterizations at each generated top-quark mass.

The likelihood function used to extract the top-quark mass includes as free parameters the number of expected signal and background b tags (n_s and n_b), and m_t. It is specified by three factors:

$$\mathcal{L}(m_t) = \mathcal{L}_{\rm sh}(m_t) \times \mathcal{L}_{n_s+n_b} \times \mathcal{L}_{\rm bkg}, \tag{1}$$

where

$$\mathcal{L}_{\rm sh}(m_t) = \prod_{i=1}^{N} \frac{n_s \cdot P_{\rm sig}(H_T^i|m_t) + n_b \cdot P_{\rm bkg}(H_T^i)}{n_s + n_b}, \tag{2}$$

$$\mathcal{L}_{n_s+n_b} = \frac{e^{-(n_s+n_b)} \cdot (n_s + n_b)^N}{N!}, \tag{3}$$

$$\mathcal{L}_{\rm bkg} = e^{-(1/2)(n_b - n_b^{\rm exp})^2/\sigma_{n_b}^2}, \tag{4}$$

and N is the number of observed b tags in the final data sample. In $\mathcal{L}_{\rm sh}(m_t)$ the product is over the number of observed b tags, and $P_{\rm sig}(H_T^i|m_t)$ and $P_{\rm bkg}(H_T^i)$ are the probability density functions for signal and background, respectively. The second factor of Eq. (1) represents a Poisson constraint on the total number of b tags observed in the data. Finally, in Eq. (4) the background normalization is constrained to its expected value $n_b^{\rm exp}$ to within $\sigma_{n_b} \equiv 10\% \cdot n_b^{\rm exp}$. The likelihood is maximized with respect to n_s, n_b, and m_t. The statistical uncertainty from the fit procedure is taken from the m_t values where the log-likelihood changes by 0.5 units from its maximum. Since we are counting b tags and not events, the H_T distribution does not strictly follow the Poisson statistics. We correct for this effect below.

We use simulated data ensembles (pseudoexperiments) to check our fitting procedure for possible systematic biases. For each generated top-quark mass from 150 GeV/c^2 to 200 GeV/c^2, we construct pseudoexperiments, with the same statistical properties as our observed data sample, by randomly sampling from the signal and background templates. Then we perform likelihood fits to each pseudoexperiment and characterize the accuracy of the technique in determining the correct m_t value. In each pseudoexperiment, the number of background b tags is Poisson fluctuated around its expectation, $n_b^{\rm exp}$, while the number of signal b tags is Poisson fluctuated around the number observed in the data, minus the central value for the background expectation. In this procedure, b tags from single and double b-tagged events are fluctuated separately. For each pseudoexperiment, the likelihood fit provides the measured m_t along with the positive and negative statistical uncertainties from which pull distributions are derived. The mean of the pull distribution, averaged as a function of the input m_t, is consistent with zero (-0.01 ± 0.02), while the width is slightly larger than unity, due to the inclusion of duplicated H_T values in the pseudoexperiment distributions in the case of double-tagged events. For the current analysis, we correct for this effect by scaling the statistical errors taken from $\Delta \ln \mathcal{L} = -1/2$. The scale factor is the pull width averaged over m_t ranging between 150 and 200 GeV/c^2, giving 1.08 ± 0.02.

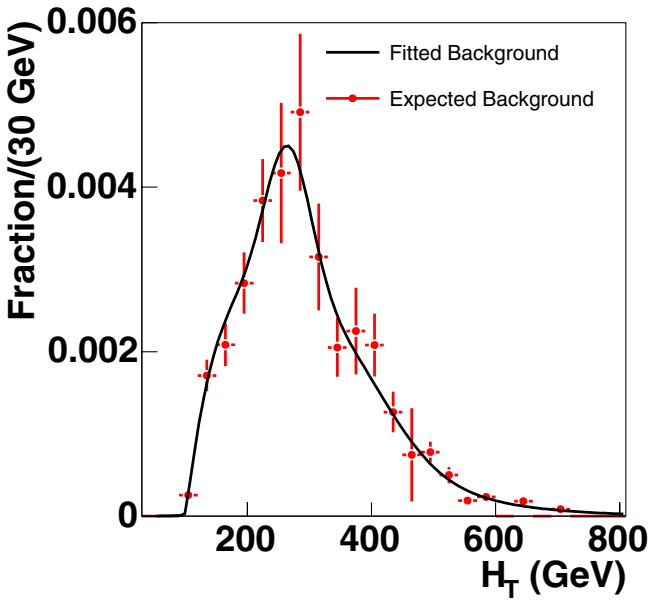

FIG. 3 (color online). The background H_T template, after the subtraction of the $t\bar{t}$ content (using $m_t = 172.5$ GeV/c^2) is shown overlaid with the fitted parameterization.

Applying our method to the observed H_T distribution, we find $n_s = 76.2 \pm 11.4$, $n_b = 54.6 \pm 5.1$, and $m_t = 172.3^{+10.8}_{-9.6}(\text{stat})$ GeV/c^2. The statistical uncertainties on m_t are consistent with expectation from pseudoexperiments performed with an input top-quark mass of 172.5 GeV/c^2. The result from the fit to the data is shown in Fig. 4. The inset shows the function $-2\ln\mathcal{L}$ from the final fit as a function of m_t.

Systematic uncertainties arise from uncertainties in our understanding of the detector response and in the assumptions employed to infer the top-quark mass from the observed data. For each source of systematic uncertainty, the relevant input quantities are varied by $\pm 1\sigma$, and new signal or background H_T templates are produced by performing the event selection and reconstruction on the modified samples. Then these new fixed templates are used to run pseudoexperiments. The mean shift in the fitted top-quark mass with respect to the input value is taken as the systematic uncertainty associated with the given assumption or effect. Table I reports all the relevant sources of systematics associated with our measurement. The dominant source of uncertainty (9.6 GeV/c^2) given the choice of H_T as discriminant variable is associated to jet energy scale uncertainty. For each jet considered in the H_T calculation, the relative jet energy scale uncertainty, which is mainly driven by uncertainties on particle response calibrations and the out-of-cone jet energy modeling, varies from 3% to 8% depending on η and p_T of the jet. We determine the impact of the jet energy scale uncertainty on our measurement using pseudoexperiments in which the nominal jet energies are varied by ± 1 standard deviations.

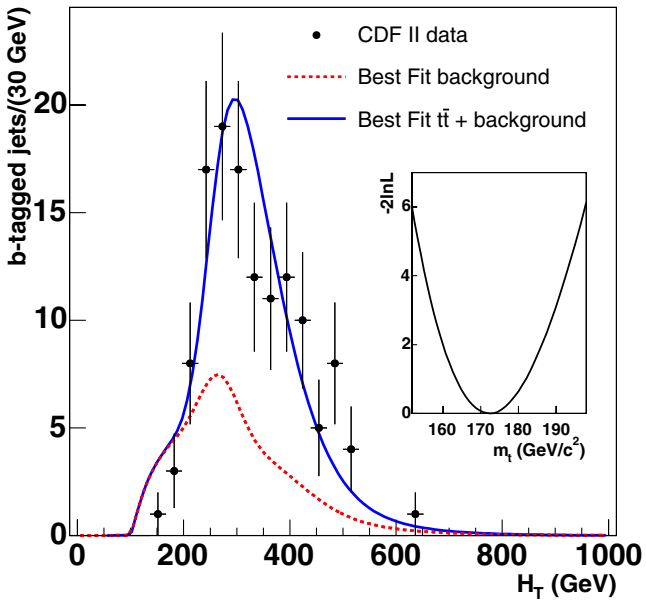

FIG. 4 (color online). H_T distribution from the selected data sample, overlaid with the expected distribution from the unbinned likelihood fit. The inset shows the $-2\ln\mathcal{L}$ from the final fit as a function of m_t.

TABLE I. Relevant sources of systematic uncertainty.

Source	Δm_t (GeV/c^2)
Jet energy scale	9.6
Generator	3.8
Background shape	2.1
PDFs	1.5
ISR	0.9
FSR	0.9
Background fraction	0.8
b-jet energy scale	0.7
Trigger efficiency	0.7
Limited Monte Carlo statistics	0.6
b tagging	0.5
Total	10.8

Additionally, the dependence on the Monte Carlo generator is estimated as the difference in the extracted top-quark mass in PYTHIA [18] and HERWIG events and amounts to 3.8 GeV/c^2. Other sources of uncertainty are related to the background shape and normalization and are evaluated to be 2.1 and 0.8 GeV/c^2, respectively. We estimate the uncertainty from PDFs using signal samples in which the events are weighted according to their probability to occur using different sets of PDF eigenvectors. The systematic uncertainty is computed by considering differences between the CTEQ5L and MRST72 [19] PDFs parameterizations, different Λ_{QCD} values, and the sum in quadrature of half the difference between the $\pm 1\sigma$ shift of the 20 CTEQ6M uncertainties, for a total of 1.5 GeV/c^2. Variation of initial (ISR) and final state (FSR) gluon radiation settings, as in [5], are found to contribute 0.9 GeV/c^2 of systematic uncertainty each. Systematic uncertainties due to the b-jet energy scale, trigger simulation effects, statistically limited Monte Carlo samples, and b-tagging efficiency modeling are small and give a combined error of 1.2 GeV/c^2. The total systematic uncertainty is estimated to be 10.8 GeV/c^2 assuming all sources to be uncorrelated.

In conclusion, we report the first top-quark mass measurement using inclusively selected $\not\!\!E_T$ + jets $t\bar{t}$ events with a large acceptance for $W \to \tau\nu$ decays. The result, $m_t = 172.3^{+10.8}_{-9.6}(\text{stat}) \pm 10.8(\text{syst})$ GeV/c^2, is complementary and statistically independent with respect to precision CDF measurements [5,6], and consequently, although not competitive by itself, it will help to reduce by a few percent the overall uncertainty on m_t when combined with other existing results.

We thank the Fermilab staff and the technical staffs of the participating institutions for their vital contributions. This work was supported by the U.S. Department of Energy and National Science Foundation; the Italian Istituto Nazionale di Fisica Nucleare; the Ministry of Education, Culture, Sports, Science and Technology of Japan; the Natural Sciences and Engineering Research

Council of Canada; the National Science Council of the Republic of China; the Swiss National Science Foundation; the A. P. Sloan Foundation; the Bundesministerium für Bildung und Forschung, Germany; the Korean Science and Engineering Foundation and the Korean Research Foundation; the Particle Physics and Astronomy Research Council and the Royal Society, UK; the Institut National de Physique Nucleaire et Physique des Particules/CNRS; the Russian Foundation for Basic Research; the Comisión Interministerial de Ciencia y Tecnología, Spain; the European Community's Human Potential Programme; the Slovak R&D Agency; and the Academy of Finland.

[1] LEP Collaborations, LEP Electroweak Working Group, and SLD Electroweak and Heavy Flavor Groups, Report No. CERN-PH-EP/2004-069.

[2] S. Heinemeyer *et al.*, J. High Energy Phys. 09 (2003) 075.

[3] W.-M. Yao *et al.*, J. Phys. G **33**, 1 (2006).

[4] The CDF II coordinate system uses θ and ϕ as the polar and azimuthal angles, respectively, defined with respect to the proton beam axis direction, z. The pseudorapidity η is defined as $\eta \equiv -\ln[\tan(\theta/2)]$. The transverse momentum of a particle is $p_T = p\sin\theta$, and the transverse energy is defined as $E_T = E\sin\theta$. The missing transverse energy, $\vec{\not\!\!E}_T$, is defined by $\vec{\not\!\!E}_T \equiv -\sum_i E_T^i \hat{\mathbf{n}}_\mathbf{i}$, where the index i runs over all calorimeter towers with $|\eta| < 3.6$, and $\hat{\mathbf{n}}_\mathbf{i}$ is a unit vector perpendicular to the beam axis and pointing at the ith calorimeter tower.

[5] A. Abulencia *et al.* (CDF Collaboration), Phys. Rev. Lett. **96**, 152002 (2006); **96**, 022004 (2006); Phys. Rev. D **73**, 032003 (2006).

[6] T. Aaltonen *et al.* (CDF Collaboration), Phys. Rev. Lett. **98**, 142001 (2007).

[7] D. Acosta *et al.* (CDF Collaboration), Phys. Rev. D **71**, 052003 (2005).

[8] Among other selections, the all-hadronic mass sample is required to have $\not\!\!E_T$ significance, $\not\!\!E_T^{\mathrm{sig}}$, less than 3.0 $\mathrm{GeV}^{1/2}$.

[9] D. Acosta *et al.* (CDF Collaboration), Phys. Rev. D **71**, 032001 (2005).

[10] A. Abulencia *et al.* (CDF Collaboration), Phys. Rev. Lett. **96**, 202002 (2006).

[11] A. Bhatti *et al.*, Nucl. Instrum. Methods Phys. Res., Sect. A **566**, 375 (2006).

[12] G. Marchesini, B. R. Webber, G. Abbiendi, I. G. Knowles, M. H. Seymour, and L. Stanco, Comput. Phys. Commun. **67**, 465 (1992).

[13] J. Pumplin, D. R. Stump, J. Huston, H. L. Lai, P. Nadolsky, and W. K. Tung, J. High Energy Phys. 07 (2002) 012.

[14] P. Avery, K. Read, and G. Trahern, CLEO Report No. CSN-212, 1985 (unpublished).

[15] E. Gerchtein and M. Paulini, Proceedings of 2003 Conference for Computing in High-Energy and Nuclear Physics (CHEP 03), La Jolla, California, 2003, pp. TUMT005.

[16] S. Agostinelli *et al.*, Nucl. Instrum. Methods Phys. Res., Sect. A **506**, 250 (2003).

[17] K. Pearson, Phil. Trans. R. Soc. A **186**, 43 (1895).

[18] T. Sjöstrand, P. Eden, C. Friberg, L. Lönnblad, G. Miu, S. Mrenna, and E. Norrbin, Comput. Phys. Commun. **135**, 238 (2001).

[19] A. D. Martin *et al.*, Eur. Phys. J. C **39**, 155 (2005).